Exp Astron (2005) 20:365–373
DOI 10.1007/s10686-006-9034-5

ORIGINAL ARTICLE

Simulated performance of dedicated Ge-strip Compton telescopes as γ-lens focal plane instrumentation

C. B. Wunderer · P. von Ballmoos · N. Barrière · S. E. Boggs · G. Weidenspointner · A. Zoglauer

Received: 1 February 2006 / Accepted: 3 March 2006
© Springer Science + Business Media B.V. 2006

Abstract With focusing of gamma rays in the nuclear-line energy regime starting to establish itself as a feasible and very promising approach for high-sensitivity γ-ray (line) studies of individual sources, optimizing the focal plane instrumentation for γ-ray lens telescopes is a prime concern. Germanium detectors offer the best energy resolution available at $\sim$2 keV FWHM at 1 MeV and thus constitute the detector of choice for a spectroscopy mission in the MeV energy range. Using a Compton detector focal plane has three advantages over monolithic detectors: additional knowledge about (Compton) events enhances background rejection capabilities, the inherently finely pixellated detector naturally allows the selection of events according to the focal spot size and position, and Compton detectors are inherently sensitive to γ-ray polarization. We use the extensive simulation and analysis package assembled for the ACT vision mission study to explore achievable sensitivities for different Ge Compton focal plane configurations as a first step towards determining an optimum configuration.

Keywords X- and gamma-ray telescopes and instrumentation · Observation and data reduction techniques: computer modeling and simulation · Compton scattering · Nucleosynthesis

CBW thanks the Townes Fellowship at UCB and NASA Grant NNG05WC28G for Support.

C. B. Wunderer (✉)
Space Sciences Laboratory, UC Berkeley, CA 94720, USA
e-mail: wunderer@ssl.berkeley.edu

P. von Ballmoos · N. Barrière · G. Weidenspointner
Centre d'Etude Spatiale des Rayonnements, Toulouse, France

S. E. Boggs · A. Zoglauer
Space Sciences Laboratory, UC Berkeley, CA 94720, USA

1. Introduction

With Laue γ-ray lenses rapidly becoming a viable path to observing the MeV universe, the scope of their study must be broadened to include viable focal-plane instrumentation in addition to the lenses themselves. The detector of choice for any nuclear astrophysics mission allows to take maximum advantage of the information encoded in the astrophysical γ-ray lines, including any Doppler broadening or Doppler shifts of lines. Germanium detectors achieve the best energy resolutions in the energy regime of primary interest ($\sim$100 keV to $\sim$2 MeV) in detectors of reasonably large volumes.

While a companion paper (Weidenspointner et al.) compares the merits and demerits of similar-size monolithic, segmented, and Compton detectors at the focus of a Laue γ-ray lens, the work presented here constitutes a first attempt at optimizing a Compton telescope focal plane.

A Compton-detector focal plane would have several advantages:

- It would have a much better capability for background rejection, since each individual photon's origin can be determined to at least a circle on the sky. If this circle does not intersect the lens' position, the photon is rejected.
- A Compton detector is inherently finely pixellated. This would also enable on-the-ground selection of source events according to current focal spot size and position. Moreover, only a detector with many pixels could hope to utilize a Laue lens' imaging (as opposed to merely concentrating) capability.
- A Compton detector is inherently sensitive to γ-ray polarization.

These advantages, of course, come at the cost of a significant increase in the number of detector channels, with correspondingly higher demands on both instrument electronics and detector cooling. A Compton focal plane could also not be designed quite as compact as a single monolithic Ge detector, and would have to contend with a somewhat higher fraction of passive material inside the detector assembly itself to support the much higher number of channels and increased detector segmentation.

Ge-strip Compton detectors are available today. The *Nuclear Compton Telescope* (NCT) balloon will ultimately be made up of twelve detectors; two such detectors have been tested extensively in the laboratory and flew on a technology-demonstration balloon flight in spring 2005 (Boggs et al.).

In order to predict a Compton telescope's performance, one first must predict source and background interactions in the detectors, and then derive from these raw events the sensitivity achievable after Compton event analysis. The comparative performance evaluation of different Compton focal plane designs discussed here leverages heavily off the toolset assembled for the *Advanced Compton Telescope* (ACT) study (Boggs et al., 2005; Wunderer, et al., 2006 in press).

2. Compton telescope primer

In Compton telescopes, each individual interaction of a photon in the detector volume is recorded separately; both interaction position and energy deposit are recorded for each hit (see Figure 1). Scatter angles and deposited energies are related via the Compton equation (Compton, 1923)

$$\cos\varphi = 1 - \frac{m_e c^2}{E_{\gamma'}} + \frac{m_e c^2}{E_{\gamma'} + E_{e'}} \tag{1}$$

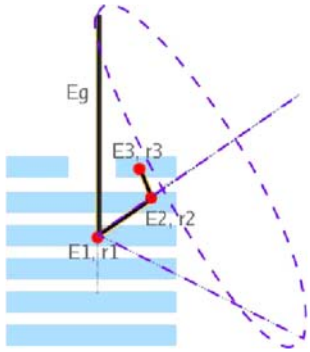

Fig. 1 Schematic of photon interactions in a Compton focal plane. In the example, the photon incident from above with energy E_g undergoes two Compton scatters before photoabsorption. The photon origin can be reconstructed to a cone.

where $m_e c^2$ denotes the rest energy of the electron, $E_{\gamma'}$ ($E_2 + E_3$ in Figure 1) the scattered photon's energy and $E_{e'}$ (E_1 in Figure 1) that of the scattered electron, and φ the angle between incident and scattered photon direction.

Using this information, the incident photon's energy and direction can be reconstructed. Measuring $E_{e'}$ and $E_{\gamma'}$ allows to calculate φ; together with the interaction positions this allows the restriction of the photon incident direction to a cone – a circle on the sky.

In this manner, of course photons recorded in the detector can be rejected if they are not consistent with the direction of the source of interest (or in this case lens) – providing a powerful tool for background reduction in addition to detector-inherent imaging capability.

3. The models

Figure 2 shows the three Compton detector designs considered. Each instrument was placed on the same generic spacecraft used for the comparison study of monolithic, segmented, and Compton stacks (Weidenspointner et al.). The detector is located at the top of a tower distancing it from the spacecraft bus and surrounded with plastic (top and sides) and BGO (bottom) anticoincidence shielding. To simulate photons from the Lens, a Laue-lens specific beam configuration was implemented; the assumed beam FWHM is $\sim 2^{\circ}$. More detail about the spacecraft model and the lens-specific input photon beam is given in Weidenspointner et al..

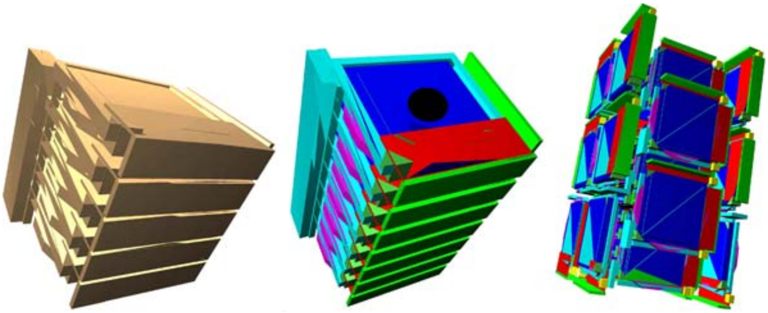

Fig. 2 Detector models considered in the comparative study of different Ge Compton focal planes. From left: small, medium, and large Compton stack. For detailed descriptions of each stack see text.

Small Compton Stack. The small Compton stack is built from 5 Ge detectors identical to those flown on the NCT balloon in Spring 2005 (Boggs et al.). The mass model faithfully represents all passive material in the existing detector assembly, as well as a cold finger and surrounding Aluminum for a cryostat. This mass model is identical to that used for the segmented and Compton stack models in the companion paper (Weidenspointner et al.).

Medium Compton Stack. For the medium Compton stack, it is assumed that the guard ring width can be reduced, that the strip pitch is reduced by a factor of two, and that the top Ge layer has a hole to allow the photons from the lens to impinge on the surface of the second detector.

Large Compton Stack. The large Compton stack makes similar assumptions as the medium one, but in addition two different thicknesses of Ge detectors are used, and the detectors are larger (available but more expensive). The aluminum bars and Ge protrusions used to mount the detectors are slimmed down within reasonable limits, resulting in a lower passive mass fraction. All the pieces required for detector mounting and operation remain part of the mass model. This stack is built from several tens of detectors. The intent was to design a photon bucket – however, the roughly circular shape of the assumed detectors leaves many "holes" through which photons can escape. Smaller, but truly rectangular detectors, together with a more careful stack design, should enable significantly more efficient assemblies than this one.

Details of the different detector concepts are summarized in Table 1. The single-detector unit model in each case is based on the current NCT Ge detector design. Basing this entire study closely on existing balloon hardware – which of course was designed with cost and reliability paramount, and minimization of passive mass a secondary consideration – ensures that the mass models are if anything overly conservative. The single-detector mass models encorporate a high level of detail. Aluminum parts clamping the detector in place, passive Germanium "handles" the clamps attach to, and circuit boards protruding between detector active areas are faithfully represented at correct composition and mass – even screws are accounted for.

There is only one spot where the mass models are too optimistic: for those detectors in the MED and LARGE concepts with a central hole, the hole is not surrounded by a guard

Table 1 Details of the three Compton Detector configurations compared in the present study

	Small	Med	Large
Configuration	5 layers	6 + 1 layer	2 + 3 thin + 4 thick + sides
Detector size	$8 \times 8\,\text{cm}^2$	$8 \times 8\,\text{cm}^2$	$9.2 \times 9.2\,\text{cm}^2$
Top hole (Diameter)	no	yes (1.9 cm)	yes (1.5 cm)
Strip width	2 mm	1 mm	1 mm
Guard ring width	2.2 mm	1.2 mm	1.2 mm
# of 1.5 cm thick det	5	7	17
# of 0.75 cm thick det	0	0	21
Total mass active Ge	2.5 kg	3.4 kg	19.4 kg
Passive mass fraction in single det. assembly	20%	20%	13%
Spacecraft mass	313 kg	315 kg	363 kg

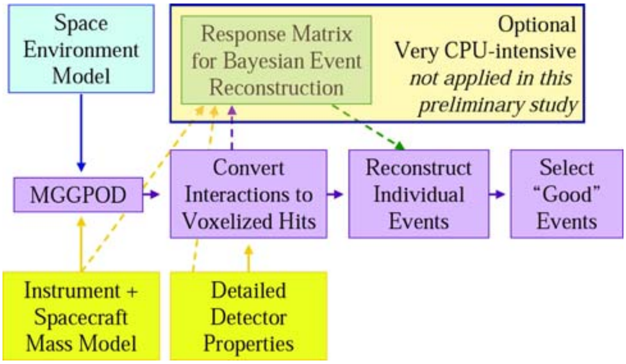

Fig. 3 Overview over the Compton data analysis steps.

ring. A real detector would require ∼1 mm guard ring there. (Constraints of the simulation toolset used made the proper implementation of a guard ring in the simulations impossible within the scope of this work.)

4. Methods

To properly assess the capabilities of any γ-ray instrument, in particular its sensitivity, an accurate evaluation of the system's susceptibility to background radiation is required. A schematic overview of the necessary steps is given in Figure 3.

4.1. MGGPOD

MGGPOD (Weidenspointner et al., 2005) is a suite of Monte Carlo codes built around the GEANT3.21 package CERN (1993) to simulate *ab initio* the physical processes relevant for the production of instrumental backgrounds at γ-ray energies. These include the build-up and delayed decay of radioactive isotopes as well as the prompt de-excitation of nuclei, both of which give rise to a plethora of instrumental γ-ray background lines in addition to continuum backgrounds. MGGPOD also comprises the GLECS (Kippen, 2004) and GLEPS (McConnell et al., 2006) packages for simulating the effects of atomic binding and polarization on photon scattering processes. Since a γ-ray lens mission would most likely require formation-flying spacecraft and therefore probably reside in a high-earth orbit or at e.g. L2, Cosmic diffuse photon (Gruber et al., 1999) and Cosmic-Ray (CR) proton spectra (Moskalenko et al., 2002) in interplanetary space were used as input background spectra (spectra are those described in Weidenspointner et al. 2005). The contribution from CR electrons (Ferreira and Potgieter, 2002; Mizuno et al., 2004) (and positrons) turns out to be negligible.

4.2. MEGAlib

The MEGAlib package (Zoglauer, 2005; Zoglauer et al., 2006 in press) was originally developed for the MEGA prototype, a tracking Compton and pair telescope consisting of a thin Si tracker and a CsI calorimeter (Kanbach et al., 2004). In the course of the ACT study, MEGAlib was enhanced to accomodate many more detector types and features, such as e.g.

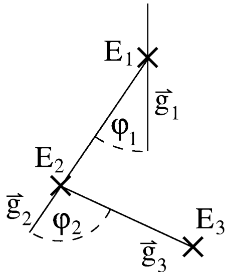

Fig. 4 Schematic illustration of a 3+ interaction Compton sequence. E_i denotes the deposited energy at interaction point i, g_i is the flight direction of the γ before the interaction, and φ_i is the Compton scatter angle.

vetoing using guard-ring readout. The package contains the complete data analysis chain for Compton telescopes, from discretizing simulation data and calibrating real measurements to the reconstruction and selection of events, up to high-level data analysis, i.e. image reconstruction, background estimation, and polarization analysis.

Event Reconstruction. The raw instrument data only gives interaction positions and energies. For n interactions, in principle $n!$ possibilities exist for the ordering of these hits – each corresponding to different possible photon incident directions. For events with *two interactions* (Compton scatter and – hopefully – subsequent photo absorption), it is very hard to discriminate between the two possible orderings except in cases for which only one order results in a valid $\cos\phi$. For this study, only two-site events were considered whose ordering could unambiguously be determined. For events with *three or more interactions*, redundant information is available that allows to determine the most likely sequence of events. The scatter angle φ_2 in Figure 4 cannot only be determined from the energy deposits using Equation (1) but also from the interaction geometry (see figure for notations):

$$\cos\varphi_2 = \frac{\vec{g_2} \times \vec{g_3}}{|\vec{g_2}| \cdot |\vec{g_3}|} \tag{2}$$

Consequently, in case of correct ordering the two evaluations of φ must agree, and the test statistics

$$T_n = \sum \left(\cos\varphi_i^{En} - \cos\varphi_i^{geo}\right)^2 \tag{3}$$

is smallest for the correct ordering. If none of the possible sequences results in a reasonably small value of T_n this is an indication that interactions are missing in the sequence – either because they happened in passive material or because the multiply-scattered photon escaped the detector. In either case the event should be rejected.

Event Selection. After reconstruction of the events, those most likely originating from the direction of interest (the lens) must be selected. Criteria include the test statistic value T_n, the Compton scatter angle φ, the number of interactions, and the minimum angular distance of the Compton cone from the source direction, the so-called Angular Resolution Measure (ARM), in addition to the total deposited energy. The event selections, i.e. data cuts, resulting in the highest instrument sensitivity to the source are determined via calculation of sensitivities for a variety of setting combinations. The optimum settings of course vary from one detector geometry to the next, and also depend on photon energy, beam shape, and source intensity.

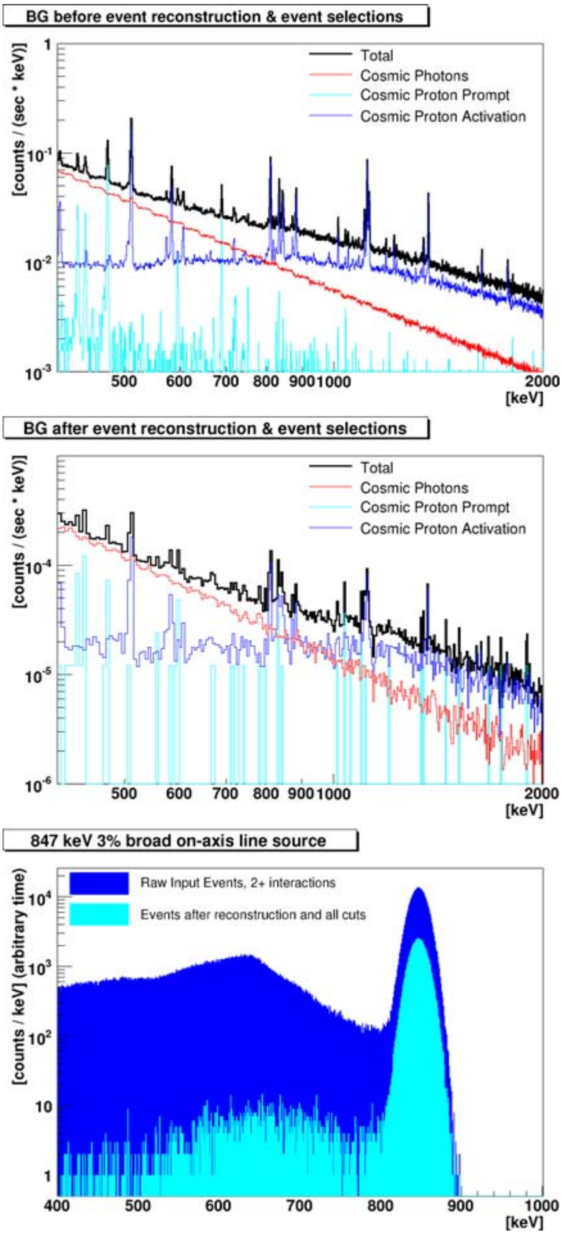

Fig. 5 Instrumental background recorded in the SMALL detector before and after event reconstruction and event selections – for comparison, a 847 keV 3% broadened source spectrum before and after the same analysis steps is also shown.

Optimum selections reject ∼75% of source counts compared to the raw detector spectrum – but well over 99% of the background events are rejected by the same selection criteria, resulting in a significant overall improvement in sensitivity. Figure 5 provides an example.

Table 2 Preliminary findings for sensitivities, efficiencies, and signal-to-background ratios. Values are *after* application of all event selections for lens effective areas of 1200 cm^2 at 511 keV and 660 cm^2 at 847 keV

	Small	Med	Large
511 keV sensitivity [ph $cm^{-2}s^{-1}$]	1.3×10^{-6}	1.2×10^{-6}	9.4×10^{-7}
847 keV sensitivity [ph $cm^{-2}s^{-1}$]	1.3×10^{-6}	1.1×10^{-6}	9.2×10^{-7}
847 keV broad-line (3% FWHM) sensitivity [ph $cm^{-2}s^{-1}$]	3.5×10^{-6}	2.7×10^{-6}	2.0×10^{-6}
Photopeak efficiency (@ 511 keV / @ 847 keV)	6%/6%	7%/6%	7%/7%
signal-to-background ratio @ 511 keV	10%	12%	13%

5. Results

Our preliminary, conservative estimates indicate that sensitivities of $1{\cdot}10^{-6}$ph $cm^{-2}s^{-1}$ for a narrow 511 keV line and $2{\cdot}10^{-6}$ph $cm^{-2}s^{-1}$ for a 3%(FWHM) broadened 847 keV line are achievable with a Laue lens of 1200 cm^2 effective area at 511 keV and 660 cm^2 at 847 keV, respectively, using a Compton focal plane. (The lens effective areas are those predicted for one version of the MAX mission's lens (Barrière et al.,).)

To appreciate this result, and the fact that this constitutes a lower limit to the capabilities of a Compton focal plane rather than a final or overly optimistic estimate, one must keep the following in mind:

– The work presented here is based on *first* guesses at good detector configurations, *no* optimization of designs has been performed yet.
– To analyze the Compton telescope data, we have used ACT analysis methods as they stand, without any optimization for the different beam as well as detector geometries in a lens focal plane.
– The detector geometries as modeled are certainly conservative, given that they reflect existing balloon hardware (NCT) rather than "what could reasonably be done". This resulted in fairly massive Aluminum mounting structures for the Ge detectors, attaching to passive Ge "handles" protruding from the detectors themselves – rather than e.g. carbon fiber frames.
– both the 511 keV electron-positron annihilation line and a broad-line region are especially demanding cases since background levels are higher than for many narrow lines at several hundred keV.

Table 2 gives more detailed simulation results for the three different Compton detector focal plane designs.

6. Conclusions and outlook

Our preliminary, conservative estimates indicate that sensitivities of $1{\cdot}10^{-6}$ph $cm^{-2}s^{-1}$ for a narrow 511 keV line and $2{\cdot}10^{-6}$ph $cm^{-2}s^{-1}$ for a 3%(FWHM) broadened 847 keV line are achievable with a Laue lens of 1200 cm^2 effective area at 511 keV and 660 cm^2 effective area at 847 keV respectively. Sensitivities achievable for narrow lines other than 511 keV should be significantly better.

A Compton detector focal plane, in contrast to the simpler monolithic or segmented approaches discussed in Weidenspointner et al., will have secondary capabilities for survey science if it is not completely enclosed by a heavy scintillator shield. At least half the sky would be visible to the Compton detector at any time. Therefore, with a Compton-telescope focal plane, a Laue-Lens instrument might detect its own targets of opportunity, and over a mission lifetime could assemble sensitive all-sky surveys.

Much remains to be done on the road to a good focal plane detector design for different mission concepts allowing different degrees of complexity for their focal planes: The compact and simplest SMALL design has little room for improvement – without changes to the individual detector's configuration, only the veto shields' geometry and the detector distance can be further optimized. The slightly more complex MEDIUM detector requires tradeoff studies for both inter-detector distances and the size of the hole in the top Ge detector, in addition to the veto shields – overall, however, it performs reasonably well.

The LARGE concept must undergo significant redesign. The initial concept that is presented here has too many gaps between the side detectors that allow scattered photons to escape to even begin to justify the significant increase in weight and complexity compared to the MEDIUM design.

Data analysis methods can be improved as well, with a corresponding improvement in expected sensitivities: The initial study presented here relies on a simple and fast analytical, instrument-independent approach to reconstructing Compton events. The currently by far most promising approach, however, is based on an extensive, highly instrument-specific response matrix and Bayesian statistics. This very computing-time intensive method has yet to be applied to the lens focal plane designs discussed in this work.

References

Barrière, N., et al.: MAX, a Laue Diffraction Lens for Nuclear Astrophysics, DOI:10.1007/s10686-006-9058-x, (2006)

Boggs, S.E., et al.: Advanced Compton Telescope vision mission study Report (2005)

Boggs, S.E., et al.: Performance of the Nuclear Compton Telescope, DOI:10.1007/s10686-006-9051-4, (2006)

CERN: Geant – detector description and simulation tool. CERN Application Software Group; Computing and Networks Division version 3.21 (1993)

Compton, A.H.: Phys. Rev. **21**(5) (1923)

Ferreira, S.E.S., Potgieter, M.S.: J. Geophys. Res. **107**, 12–1 (2002)

Gruber, D.E., et al.: Astrophys. J. **520**, 124 (1999)

Kanbach, G., et al.: New Astronomy Review **48**, 275–280 (2004)

Kippen, R.M.: New Astronomy Review **48**, 221–225 (2004)

McConnell, M., et al.: Astrophys. J. (2006) in prep.

Mizuno, T., et al.: Astrophys. J. **614**, 1113–1123 (2004)

Moskalenko, I.V., et al.: Astrophys. J. **565**, 280 (2002)

Weidenspointner, G., et al.: Monte Carlo Study of Detector Concepts for the MAX Laue Lens Gamma-Ray Telescope, DOI:10.1007/s10686-006-9035-4, (2006)

Weidenspointner G., et al.: Astrophys. J., Suppl. Ser. **156**, 69 (2005)

Wunderer, C.B., et al.: The ACT Vision Mission Study Simulation Effort. In: Proc. Astronomy with Radioactivities V. Elsevier (2006, in press)

Zoglauer, A.: First Light for the Next Generation of Compton and Pair Telescopes. PhD thesis, Technical University Munich (2005)

Zoglauer, A., et al.: MEGAlib – the Medium Energy Gamma-Ray Astronomy Software Library. In: Proc. Astronomy with Radioactivities V. Elsevier (2006, in press)